PERGAMON

International Journal of Heat and Mass Transfer 45 (2002) 3477–3489

International Journal of HEAT and MASS TRANSFER

www.elsevier.com/locate/ijhmt

Characterization of frictional pressure drop for liquid flows through microchannels

J. Judy, D. Maynes *, B.W. Webb

Department of Mechanical Engineering, Brigham Young University, 435 CTB, Provo, UT 84602, USA

Received 10 January 2002; received in revised form 8 February 2002

Abstract

This paper investigates pressure driven liquid flow through round and square microchannels fabricated from fused silica and stainless steel. Pressure drop data are used to characterize the friction factor for channel diameters in the range 15–150 μm and over a Reynolds number range 8–2300. Distilled water, methanol, and isopropanol were used in this study based on their distinct polarity and viscosity properties. Distinguishable deviation from Stokes flow theory was not observed for any channel cross-section, diameter, material, or fluid explored. © 2002 Published by Elsevier Science Ltd.

1. Introduction

Fluid flow in microtubes and microchannels has emerged as an important area of research. This has been motivated by their proposed use in such diverse applications as micropower generation, biomedical use, computer chips, and chemical separations processes. Advances in microelectro-mechanical systems (MEMS) and other microtechnologies involving fluid transport require the use of microfluidic components, which are often interconnected by tubes and channels. Quantifying the flow physics of pipe and channel flows is thus critical in understanding the momentum, heat, and mass transport characteristics at the microscale. However, only limited prior work has appeared in the literature exploring pressure-driven liquid flows through such geometries, and the results vary widely.

One of the simplest methods in exploring the validity of macroscale flow theory regarding momentum transport is to conduct pressure drop experiments over a known length of channel or capillary. For incompressible flow through horizontal pipes or channels of constant cross-sectional area, the pressure differential can be expressed as follows

$$\Delta P = \frac{\rho V^2}{2}\left[f\frac{L}{D} + \sum K_{\mathrm{L}}\right], \tag{1}$$

where f is the friction factor, ρ is the fluid density, V is the average velocity, L is the channel or tube length, D is the hydraulic diameter, and $\sum K_{\mathrm{L}}$ represents the sum of minor losses due to the inlet, exit, and hydrodynamic development length. The above expression can be solved for f and the product fRe is expressed as

$$fRe = \frac{\pi}{2}\frac{\Delta P D^4}{Q\mu L} - \frac{4}{\pi}\frac{\rho Q}{L\mu}\sum K_{\mathrm{L}}, \tag{2}$$

where Q is the fluid volumetric flow rate and μ is the dynamic viscosity. The product of the measured friction factor and Reynolds number can then be compared to the theoretical value for laminar flows (64 for circular channels). For flows in ducts of non-circular cross-section, a relationship of the form $fRe = C$ exists, where C is a constant dependent only on the channel geometry. This has been the standard approach of most experimental studies in this area. Measurements of f and Re are made, and the product fRe is then compared with the corresponding constant obtained from macroscale laminar flow theory.

* Corresponding author. Tel.: +1-801-378-3843; fax: +1-801-378-5037.

E-mail address: maynesrd@et.byu.edu (D. Maynes).

0017-9310/02/$ - see front matter
PII: S0017-9310(02)00076-5

Nomenclature

C	friction constant	Q	volumetric flow rate
D	hydraulic diameter	Re	Reynolds number ($\rho VD/\mu$)
f	friction factor	u	uncertainty in measured variable
K_L	minor loss coefficient	V	fluid average velocity
L	microchannel length	ρ	fluid density
P	pressure	μ	fluid dynamic viscosity

Recently, discrepancies between microchannel flow behavior and macroscale Stokes flow theory have been summarized in a review by Ho and Tai [1]. It is widely accepted that the deviation observed in gas flows can be attributed to slip at the wall [2] and several researchers have reported results for gas flows [3–7]. However, wall slip is not justified in explaining the observed deviations observed in incompressible flows. For laminar, incompressible flow through microtubes, prior work has reported both significant increases [8–10] and decreases [11–13] in the pressure drop from the expected value based on macroscale flow theory. Other investigations have shown no apparent deviation [14–16]. Still other investigations have reported increases in fRe for some geometries but decreases in fRe for other geometries [17,18] and some investigations have reported channel aspect ratio effects on the measured value for fRe [19,20]. Table 1 summarizes the results from 11 different studies of liquid flow through microtubes or microchannels. Note from the table that, with the exception of the work by Peng et al. [17,18], deviations in fRe have only been reported for hydraulic diameters smaller than 100 μm. The work by Peng and coworkers, however, may be held in question since the behavior of their data is so dramatically different from all other investigators using similar fluids, tube materials, and Reynolds numbers, and from Stokes flow theory.

Several theories have been presented in an attempt to explain the observed deviation from macroscale behavior, but an unquestionable conclusion has not yet been reached. For example, Mala et al. [10] propose that the product fRe should increase due to the existence of the electric double layer (EDL) and resulting streaming potential, which leads to greater frictional loss. If this assertion is correct, the product fRe should deviate more significantly as the channel hydraulic diameter decreases, since the ratio of the Debye length to diameter will increase. Also, Kulinsky et al. [21] propose a model based on the electrokinetic retardation of polar liquids, which suggests that fluids with greater polarity will experience greater frictional resistance. Another model based on micropolar behavior of liquids has been proposed by Papautsky et al. [9] which also predicts an increase in frictional resistance. No adequate theory exists in the literature to explain why the product fRe may be smaller than that predicted by Stokes flow theory, as observed in some previous investigations.

The focus of this paper is to present results of a comprehensive experimental investigation of liquid flow through microtubes and microchannels, and to discuss the experimental difficulty in accurately making such measurements. Further, the experimental data will be compared to Stokes flow theory and to previously presented results. Possible reasons for the large disparity in the differing data sets will also be proposed. Specifically, this investigation explored parametrically the following: two different channel materials (stainless steel and fused silica), hydraulic diameters of nominal size 15, 20, 30, 40, 50, 75, 100, 125, and 150 μm, a range of Reynolds number for each diameter, round and square channels, different length channels for the same channel diameter, and three liquids of very different polarity (water, methanol, and isopropanol). For liquid flow no one single study, using the same experimental apparatus, has addressed all of the issues investigated by the present work.

2. Experimental apparatus and procedure

The experimental approach taken in this study involves imposing a pressure drop across a tube of known diameter and length. The resulting liquid flow rate is also measured. From the measurement of imposed pressure drop, flow rate, tube length and diameter, and fluid properties the friction factor-Reynolds number product may be calculated according to Eq. (2). This section summarizes the experimental apparatus and procedure used in the study. This will be followed by a detailed analysis of the uncertainty in the experimental data.

A pressure source supplies fluid at known pressure, driving liquid through a microtube mounted between an upstream reservoir and a downstream collection cylinder. The pressure source used was a high-pressure syringe pump driven by a stepper motor operated in constant pressure mode. The pump, which is capable of pressures as high as 16.2 MPa (160 atm), maintained pressures constant over each test to within the uncer-

Table 1
Summary of friction results of 11 different investigations of liquid flow through microtubes and micro channels

Study	Channel/tube material	D (μm)	Fluid	Re	Observed deviation from Stokes flow theory
Urbanek et al. [8]	Silicon channel	12, 25	1–2 Propanol, 1-3 Pentanol	NA	5–30% increase in fRe; dependent on fluid temperature
Papautsky et al. [9,19]	Metallic channel	44, 57	Water	0.001–120	10–20% increase in fRe
Mala et al. [10]	Silicon	51–169	Water	0–1500	0–40% increase in fRe
Pfahler et al. [11]	Silicon channel	0.5–40	Isopropanol, silicon oil	< 100	0–30% decrease in fRe with fluid type, channel diameter; Re dependence observed
Yu et al. [12]	Fused silica circular tube	52	Water	300–2000	19% decrease in fRe
Jiang et al. [13]	Silicon channel	35–120	Water	1–30	50–100% decrease in fRe
Harms et al. [14]	Silicon channel	403	Water	125–1500	Good agreement with Stokes theory
Pfund et al. [15]	Silicon channel	200–900	Water	40–1300	Good agreement with Stokes theory
Webb and Zhang [16]	Silicon channel	133	R-134a	Turbulent	Good agreement with macroscale empirical turbulent flow data
Peng and Peterson [17]	Stainless steel channel	133–143	Water	100–3000	fRe increased for some diameters, decreased for other; dependent on Re
Peng et al. [18]	Stainless steel channel	133–367	Water	100–800	fRe increased for some diameters, decreased for others; dependent on Re

tainty of the pressure measurement. The pump reservoir was connected by small-diameter stainless steel tubing to a plenum just upstream of the microtube sample. The plenum diameter was designed with a cross-sectional area over 100 times that of the largest microtube sample tested, assuring that the fluid velocity in the plenum was negligibly small. A calibrated pressure transducer (Omega PX202) was used to measure the pressure in the plenum. The transducer output voltage was linear with applied pressure over its operating range to a maximum of 34 MPa. The uncertainty in pressure measurement was 0.25% of the maximum reading. The transducer was zeroed prior to, and confirmed following each test.

Fused silica and stainless steel microtubes of circular cross-section, and fused silica microchannels of square cross-section were mounted for flow testing between the plenum and the downstream collection reservoir. Each microtube sample was mounted with high-pressure Swagelok fittings using vespel ferrules to eliminate leakage. The fluid flow in the microtube exited to a 10 ml graduated cylinder reservoir where the fluid level was always maintained above the tube exit so as to eliminate surface tension forces at the microtube exit. The fluid at the top of the graduated cylinder was exposed to the atmosphere. The maximum hydrostatic pressure of the fluid column in the graduated cylinder was less than 0.05% of the minimum pressure difference imposed across the microtube, and was therefore neglected.

The fluid flow rate for a given pressure difference and microtube sample was determined by collecting a liquid volume over a corresponding measured elapsed time. All of the tests were conducted with an incremental added volume of at least 5 ml. The measurement was initiated after the pump initial pressure was set and the fluid began flowing, and after the fluid level in the graduated cylinder reached a pre-set minimum. The elapsed time was then recorded when the level in the cylinder reached the desired incremental increase. The least count in the graduated cylinder was 0.1 ml.

Many tests required long time periods to collect the 5–6 ml of liquid desired. To characterize the effect of evaporation from the liquid free surface over the test time, a graduated cylinder identical to that used as exit reservoir in the flow experiments was filled with each of the three fluids tested. The recession of the liquid free surface was recorded as a function of time, from which the evaporation rate was calculated. There was no detectable evaporation for either the water or methanol. The evaporation rate for isopropanol, which is considerably more volatile than either of the other two fluids, amounted to 2.5% of the microtube flow rate in the worst case (lowest tube flow rate). Evaporation rates for the isopropanol of less than 1% of the microtube flow rate were more representative for the majority of the tests. Despite determining that the evaporation rates were negligible, a stopper (with a small opening to prevent pressurization) was placed on top of the collection cylinder during every test that required longer than approximately 10 min. The stopper effectively eliminated the evaporation of the fluid.

Precise liquid temperature measurements were necessary in determining accurate values for viscosity and density. A K-type thermocouple was placed in the exit reservoir of the test setup to measure the exit temperature of the flow. Another thermocouple was attached to a brass fitting just upstream of the microtube inlet. The thermocouple was insulated, and since the thermal conductivity of the brass fitting is high, the thermocouple measurement was an accurate representation of the inlet liquid temperature. Temperature measurements were taken at the beginning and end of each test run at both the inlet and outlet. These temperature values were then averaged to determine a representative average temperature for the fluid. The thermocouples were accurate to approximately 1 °C. Due to viscous heating, the difference between inlet and outlet temperature was observed to increase with increasing velocity, but never exceeded 6°C for any test [22]. The effect of viscous heating will be explored in more detail in a later section. The uncertainty in the temperature measurement was estimated to be one half of the difference between the maximum and minimum temperature for each test. Thermophysical properties were determined from the DIPPR thermophysical property database for the fluids tested [23].

Commercially available fused silica and stainless steel tubes of circular cross-section, and fused silica microchannels of square cross-section were investigated. The fused silica tubes and channels were obtained from Polymicro Technologies and the stainless steel tubes were obtained from the Microgroup. The fused silica and stainless steel circular tubes had outside diameters of approximately 375 μm and 300 μm, respectively, regardless of inside diameter. Nominal inside diameters of the circular cross-section tubes tested ranged from 15 to 150 μm. Each tube was cut to a desired length in order to permit frictional pressure drop characterization over a specified Reynolds number range, dictated by the capacity of the high-pressure pump. The protective polyimide coating on the fused silica microtubes was scored and the tubes easily and cleanly broken. The stainless steel tubes were cut and de-burred using an electrochemical saw. The tested length of each microtube was reduced with decreasing diameter to allow for less pressure drop along the tube, permitting testing at higher Reynolds numbers. The smallest sample length to facilitate proper installation in the test setup fixtures was approximately 3.8 cm. A linear rule with least count of 0.64 mm was used for all of the microtube length measurements.

It should be noted here that a unique microtube sample was used for each of the different fluids tested. This practice was followed to prevent any long-term

fluid-tube interactions (liquid absorption at the tube wall, etc.) that might have skewed tests with a different fluid in the same microtube sample. Further, the syringe pump reservoir and associated fluid delivery system were purged three to four times with the new fluid when testing was initiated with a different liquid.

A scanning electron microscope (SEM) was used to inspect and measure the inside diameter of each microtube sample. The fused silica tubes were sputter-coated with a 1–3 nm thickness of gold. The low-voltage SFEG SEM system permitted imaging of the coated fused silica tubes without "charging," a phenomenon exacerbated at high voltages which blurs feature boundaries in the SEM images. Representative scanning electron micrographs of the fused silica circular and square cross-section microchannels, and stainless steel circular cross-section microtubes tested are shown in Figs. 1–3, respectively The fused silica microtubing featured smooth walls with few wall perturbations. By contrast, the stainless steel microtubes featured significant wall irregularities. An SEM measurement standard was acquired (Geller Microanalytical Laboratory) to calibrate the SEM for tube diameter measurements. The calibration standard was accurate to ±1%. Using the same SEM voltage and magnification as that used for each microtube sample, the calibration standard was measured. SEM magnifications ranging from 450 to 2200 times were used. The microtube sample diameters were then adjusted based on the calibration standard measurement.

Eight diameter measurements were made along different diametral lines, tracing user-specified lines in the SEM imaging utility from one tube wall tangent to a corresponding tangent on the opposite side. The side-length of the fused silica square microchannels was measured similarly by taking eight measurements along perpendicular axes. The measurement procedure for all microtubes, circular and square, was performed for both the inlet and exit. The wavy surface of the stainless steel microtubes made accurate diameter characterization challenging, as will be reflected in the diameter uncertainty for the stainless steel samples. The 16 measurements (eight each at the tube inlet and exit) were averaged to minimize the measurement error. Inlet and exit measurements were also used to quantify the variation of tube diameter along the sample length. The difference between the average of the inlet and exit diameter measurements was small for all microtubes. The fused silica circular and square microtubing exhibited differences between exit and inlet diameters of between 0.14% and 0.86%, and 0.11% and 0.33%, respectively. As might be expected, the stainless steel microtubes yielded the greatest variance in measured diameter, with differences between average inlet and exit diameters ranging from 1% to 2%.

The uncertainty in microtube diameter measurement is comprised of several contributions. The minimum uncertainty in all measurements is the ±1% error in the SEM calibration standard. There is additional uncertainty due to the variation in diameter measurements for the multiple diametral lines at both inlet and exit. The uncertainty in diameter due to variation in multiple measurements may be quantified as twice the standard deviation, for 95% confidence. The standard deviations of the multiple measurements for the fused silica circular, fused silica square, and stainless steel circular microtubes were in the range 0.31–0.83%, 0.41–0.70%, and 1.29–2.53%, respectively. Finally, there may be some human bias in the selection of tangent locations, etc.

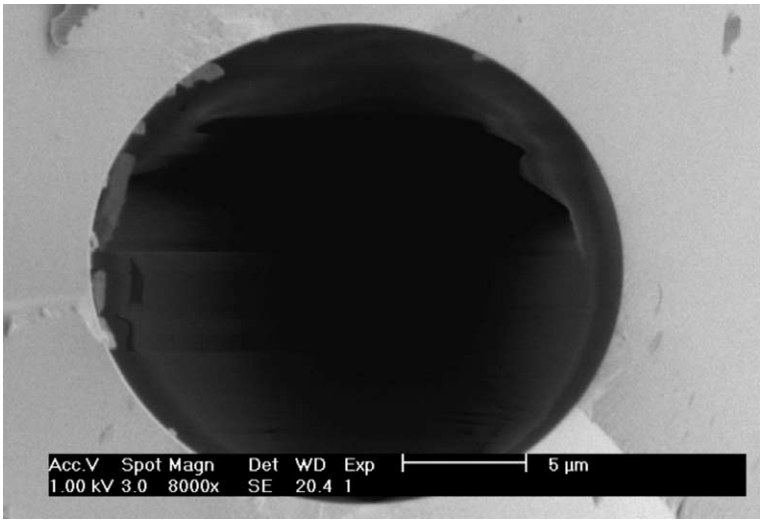

Fig. 1. SEM image of the cross-section of a fused silica circular microtube with a nominal internal diameter of 22 μm.

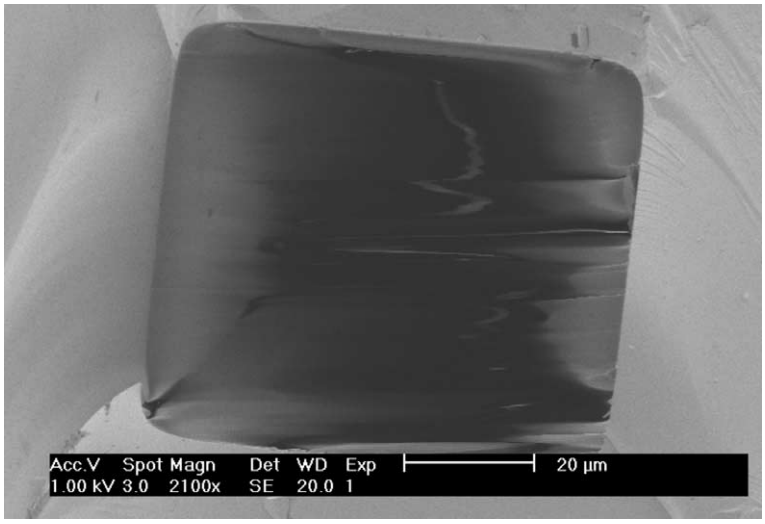

Fig. 2. SEM image of the cross-section of a fused silica square microchannel with a nominal internal diameter of 50 μm.

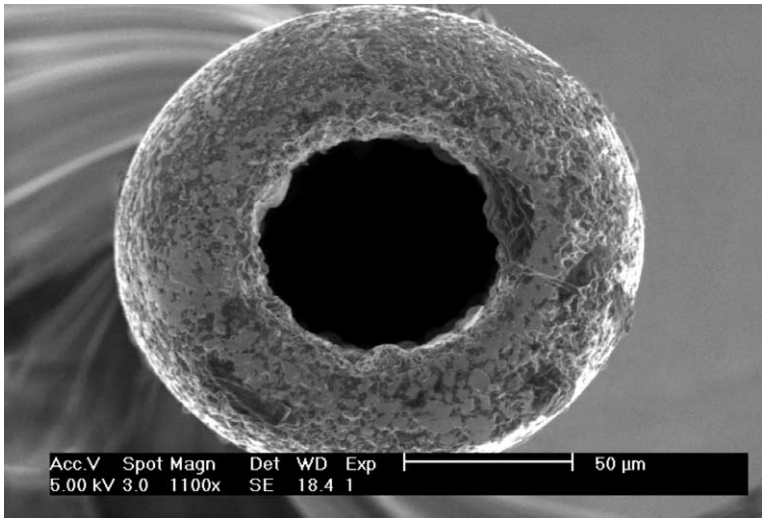

Fig. 3. SEM image of the cross-section of a stainless steel circular tube with a nominal internal diameter of 75 μm.

This human bias is difficult to quantify, and can only increase the overall uncertainty in diameter measurement. It may be said, therefore, that the minimum uncertainty in diameter for each sample is the sum of error in the calibration standard and the random error in the multiple measurements (twice the standard deviation for 95% confidence). Conservatively, the minimum uncertainty in diameter for the fused silica circular, fused silica square, and stainless steel circular microtubes is estimated to be 2.5%, 2.5%, and 5.0%, respectively. As will be shown in the overall uncertainty analysis to follow, these values are quite critical.

It is instructive to characterize the effect of minor losses on the overall pressure drop in the microtube. Accepted loss factors for laminar flow re-entrant duct entrance ($K_L = 0.8$), abrupt exit ($K_L = 1.0$), and hydrodynamic development length ($K_L = 1.3$) were used in accounting for the minor losses in the tube [24]. The largest contribution that the minor losses had in all test data sets was 3.7% of the total ΔP. This occurred at the highest Reynolds number with water in the 125.4 μm stainless steel tube. For tests in fused silica tubing the minor losses were less than 3% of the overall ΔP for all tests and all fluids. For all data taken in tubes of di-

ameter less than 75 μm, the sum of minor losses was less than 1% of the overall pressure drop.

Establishing liquid flow in microtubes requires a significant inlet pressure. The elevated pressures required to achieve these flows may affect the properties of the fluids. The bulk modulus of elasticity for water, isopropanol, and methanol is 2.15×10^9 N/m^2, 1.2×10^9 N/m^2, and 8.3×10^8 N/m^2 respectively [25]. Thus, the maximum change in density for all tests and for all three fluids was 1.9%; typical density changes were much less than 1%. The viscosity of liquids is also known to increase with pressure. However, the only characterization of the effect for water, isopropanol, and methanol appears to be a 1926 work by Bridgman which reports measurements of the viscosity's dependence on pressure at *ultrahigh* pressures (as high as 12,000 atm) [26,27]. The lowest elevated pressure tested in that study was 500 atm. For water, the effect of pressure on viscosity is shown to be very small (estimated to be less than 0.5% for the pressure range of this study). Although extrapolating the ultrahigh pressure viscosity data of Bridgman to the much lower pressures investigated in the present study (160 atm) is questionable, the result suggests that the viscosity for isopropanol may change by as much as 10–15% at the maximum pressure of this study. The extrapolated maximum change for the viscosity of methanol is 5–7%. Given the apparent inapplicability of Bridgman's property data to the pressure range of this study, no pressure correction to viscosity was applied. An increase in liquid viscosity with pressure would manifest itself as a decreasing trend in fRe with increasing pressure drop (increasing Re). As will be shown later, such a trend is not evident in the data of this study. Further, it is unclear whether the effect of pressure on viscosity has been addressed in previous work.

It is possible that diffusion of air into the liquids being tested could alter the flow characteristics, particularly at this physical scale. To minimize the possibility of gas adsorption by the fluids, each fluid was stored in an air-tight container and opened only to fill the syringe pump. Further, a test was performed to characterize the influence of dissolved gases on the pressure drop measurements for distilled water. Eight measurements at different Reynolds numbers were taken with distilled water that had been boiled for five continuous minutes at room temperature by lowering the pressure with a vacuum pump. The average measured fRe value for these eight points was within 2.2% of the average for measurements made with non-boiled liquid. It was concluded that the effects of gasification on the flow properties were negligible for this study.

Tests were conducted at identical experimental conditions on multiple occasions to assess the repeatability of the data. For the few select experimental conditions for which repeatability was investigated, the data were replicated to within 1%.

3. Experimental uncertainty

A careful analysis of the experimental uncertainty in this study is critical to the interpretation of experimental data and exploration of deviation from macroscale theory. Using accepted error analysis, the uncertainty associated with a parameter as a function of other measured variables $p(\sigma_1, \sigma_2, \sigma_3, \ldots, \sigma_n)$ may be stated as

$$u_p = \sqrt{\sum_{i=1}^{n} \left(\frac{\partial p}{\partial \sigma_i} u_{\sigma_i} \right)^2}, \tag{3}$$

where u_p is the uncertainty in the parameter p, σ_i are the variables of functional dependence, and u_{σ_i} is the uncertainty in the measurement of each functional dependence variable σ_i. Applied to the friction factor-Reynolds number product relation of Eq. (2), the uncertainty in fRe may be expressed as

$$\begin{aligned} u_{fRe} = \frac{\pi}{2} \frac{\Delta P D^4}{\mu Q L} \Bigg\{ & \left(\frac{u_{\Delta P}}{\Delta P} \right)^2 + \left(4 \frac{u_D}{D} \right)^2 \\ & + \left(1 + \frac{Re}{C} \frac{D}{L} \sum K_{\mathrm{L}} \right)^2 \left(\frac{u_Q}{Q} \right)^2 \\ & + \left(1 - \frac{Re}{C} \frac{D}{L} \sum K_{\mathrm{L}} \right)^2 \left[\left(\frac{u_\mu}{\mu} \right)^2 + \left(\frac{u_{\mathrm{L}}}{L} \right)^2 \right] \\ & + \left(\frac{Re}{C} \right) 2 \left(\frac{D}{L} \right)^2 u_{K_{\mathrm{L}}}^2 \Bigg\}^{1/2}, \end{aligned} \tag{4}$$

where C is the Stokes (macroscale) flow value of fRe for the tube of interest (i.e., in laminar flow $C = 64$ for circular tubes, 56.9 for square tubes). Presuming that a hydrodynamic fully-developed condition exists (as will be documented for the experimental data of this study in a section to follow), Eq. (4) may be simplified for large L/D in laminar flows ($Re < 2000$). For the dimensionless tube aspect ratios ($1203 < L/D < 5657$) and Reynolds number range ($8 < Re < 2431$) explored in this study, the contributions to uncertainty due to minor losses in Eq. (4) may be neglected (incurring less than 0.05 absolute percentage points in the overall error calculation), and the expression for fractional uncertainty in fRe becomes

$$\begin{aligned} \frac{u_{fRe}}{fRe} = \Bigg[& \left(\frac{u_{\Delta P}}{\Delta P} \right)^2 + \left(4 \frac{u_D}{D} \right)^2 + \left(\frac{u_Q}{Q} \right)^2 + \left(\frac{u_\mu}{\mu} \right)^2 \\ & + \left(\frac{u_{\mathrm{L}}}{L} \right)^2 \Bigg]^{1/2}. \end{aligned} \tag{5}$$

Eq. (5) shows clearly that the experimental uncertainty in fRe is dominated by the error in the measurement of

tube diameter D, since the uncertainty in diameter is multiplied by a factor 4. This suggests that despite the extreme care exercised in measuring the tube diameters with the calibrated SEM, the *minimum* uncertainty in fRe for the fused silica circular, fused silica square, and stainless steel circular microtubes (as dictated by uncertainty in diameter) is 10%, 10%, and 20%, respectively. Using Eq. (4) to include error contributions from all measured parameters, u_{fRe}/fRe for the fused silica circular, fused silica square, and stainless steel circular microtubes lie in the range 10.2–15.0%, 10.3–11.4%, and 20.2–21.4%, respectively. Any deviation in observed frictional pressure drop from the macroscale theory must therefore exceed these uncertainty limits in order to be statistically detected.

4. Test matrix

A comprehensive experimental study using three liquids (distilled water, isopropanol, and methanol) with two different tube materials (fused silica and stainless steel) for two different channel cross-sections (circular and square), over a large range of microtube hydraulic diameters was formulated. This parametric set was designed to explore frictional pressure drop at the microscale for polar and non-polar fluids, electrically conducting and dielectric tubes, for two tube cross-section geometries. Tube hydraulic diameters ranging from 15 to 150 μm were investigated, spanning the range where deviation from macroscale theory has been reported in prior work. Measurements were also taken for a fixed tube material and diameter at several different tube lengths, to confirm the existence of a fully developed condition. A typical data set for one tube configuration consisted of approximately 15–20 flow rates spanning the full range of Re permitted by the pump capacity. The possible range at the lowest microtube diameter (15 μm) was severely restricted by pump capacity. Table 2 summarizes the nominal microtube (hydraulic) diameters, tube lengths, and Reynolds number ranges investigated. All tube configurations were tested with three fluids-distilled water, isopropanol, and methanol. The dielectric constants of distilled water, methanol, and isopropanol are, respectively, 80.37, 33.6, and 18.3 [28]. Distilled water is very polar as compared to isopropanol, which is characteristically non-polar. The polarity of methanol lies between these two extremes. The data for circular and square cross-section microtubes were collected to study geometry effects and to compare the results to the microchannel test results found in the literature.

Table 2
Range of experimental parameters investigated. All tests were conducted with the three fluids investigated, distilled water, methanol, and isopropanol

D (nominal, μm)	L (m)	Re
Fused silica circular microtubing		
15	0.036	34–41
20	0.030–0.050	18–989
30	0.040–0.070	8–1716
40	0.050–0.37	17–769
50	0.070–0.29	44–1451
75	0.30–0.39	146–1883
100	0.30	109–1858
150	0.20–0.30	137–1540
Fused silica square microtubing		
50	0.080–0.13	61–1527
75	0.11–0.30	161–1150
100	0.18–0.30	95–1723
Stainless steel circular microtubing		
75	0.15	83–2384
100	0.18	66–2431
125	0.30	58–1800

5. Results and discussion

The existence of a hydrodynamically fully-developed condition in microtube flows has been questioned. A number of experiments were performed using tubes of the same nominal diameter but for different tube lengths. Results are presented in Fig. 4 for water flow in fused silica microtubes of diameters ranging from 22 to 149 μm. Each data point represents pressure drop data taken at the maximum Reynolds numbers for a given tube diameter and length. The maximum Reynolds number was chosen for presentation in the figure, since for the higher Reynolds number, the development length is expected to be the greatest. The figure shows clearly that to well within the uncertainty of the experimental data, fRe is independent of L/D for all diameters tested. This

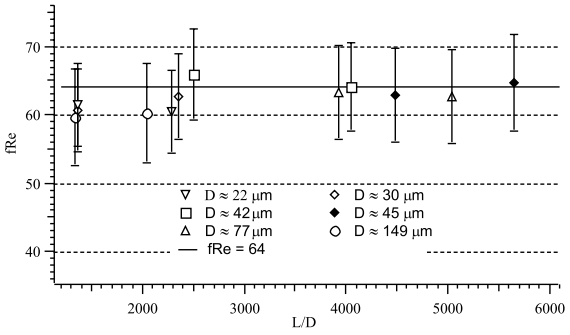

Fig. 4. Measured fRe as a function of dimensionless tube length L/D for distilled water.

suggests that a hydrodynamically fully developed flow condition exists over the majority of the microtube length, since no change in frictional pressure drop parameter is evident with changing length of the same diameter.

It will be noted that for some fluids, viscous dissipation can affect the development length in tubes at this physical scale, particularly at higher average fluid velocities. The influence of viscous dissipation was explored for the data collected here, and as possible sources for the deviation from Stokes flow behavior repeated in previous work. Viscous heating has the effect of increasing the temperature of the flowing fluid along the tube axis, yielding continuously varying thermophysical properties. The Nahme number is used to estimate the importance of viscous dissipation [29]. For pipe flow the Nahme number is defined as

$$Na = -\frac{4\beta\mu}{k}V^2, \tag{6}$$

where β is the temperature sensitivity of viscosity defined as $-(1/\mu)(\partial\mu/\partial T)$, μ is the viscosity, k is the thermal conductivity, and V is the average fluid velocity in the tube. The temperature sensitivity of viscosity may be found in standard property databases [25,30]. Viscous dissipation effects become significant for increasing Na. For the liquids and Reynolds number ranges used in this study, the largest Nahme number for the presented data was 0.02, and was found for the isopropanol. This small Na suggests that for the data presented in this study the viscous dissipation effects were small. Despite this small Na, viscous heating of the fluid can affect the results. As has been previously indicated, liquid temperatures were measured both at the inlet and the exit of the microtube. Fig. 5 illustrates fRe as a function of Reynolds number for a fused silica square microchannel of length $L = 11.4$ cm and hydraulic diameter $D = 74.1$ μm ($L/D = 1543$) with isopropanol as the working fluid. The maximum rise in liquid temperature for this case was 6.2 °C, found at the maximum Reynolds number tested $Re \approx 300$. The figure shows fRe calculated two ways: (i) using a viscosity based on the tube inlet temperature, and (ii) using a viscosity based on the average of tube inlet and exit temperatures. Faired curves are drawn through both data sets to reveal trends. Note that when the average temperature is used fRe is effectively independent of Reynolds number. By contrast, when the temperature at the tube *inlet* is used to evaluate the viscosity, the friction factor drops with increasing Reynolds number as the effect of viscous heating becomes more pronounced at higher fluid velocities. Even for the small Nahme number characterizing this data set ($Na = 0.02$), the viscous heating and associated viscosity variation can result in a 7–10% drop in fRe. For the small Nahme numbers and associated small rise in mean temperature over tube length found in tests reported here, the average of the fluid temperatures at the tube inlet and exit appears to be an appropriate reference condition on which to base thermophysical properties. All data shown hereafter were calculated using properties evaluated at the average temperature. If even small temperature rises due to viscous heating are not properly accounted for, errors can occur in reported friction factors. Variations in fRe with varying Reynolds number is a phenomenon reported previously [17,18], and may or may not be related to viscous heating.

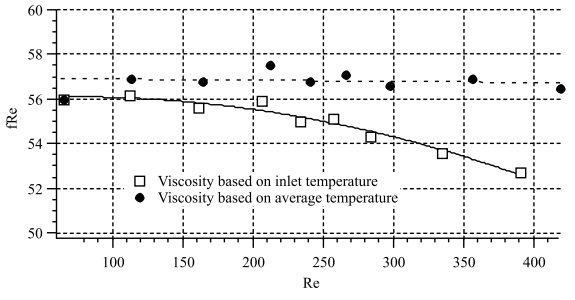

Fig. 5. Measured fRe versus Reynolds number with viscosity based on: (i) average tube fluid temperature and (ii) inlet temperature for a fused silica square microchannel with isopropanol.

The most extensive data set was that obtained using fused silica circular tubing. The friction factor-Reynolds number product is shown as a function of Reynolds number for the fused silica circular microtubes in Figs. 6–8 for the distilled water, isopropanol, and methanol, respectively. The value of fRe remained approximately constant over the entire Reynolds number range studied for all diameter/fluid test combinations. The greatest standard deviation for fRe data over the range of Re investigated for fixed diameter, length, and for all fluids

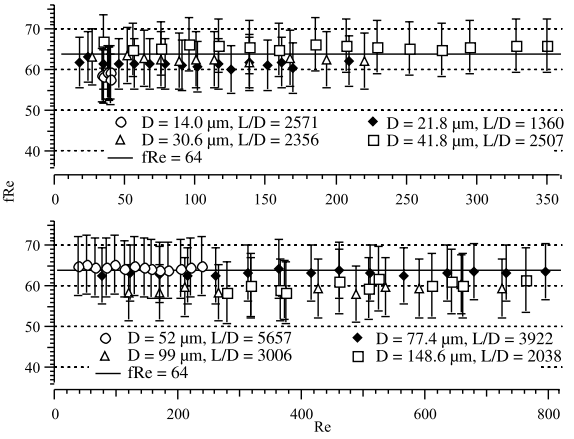

Fig. 6. Measured fRe as a function of Reynolds number for fused silica circular microtubes with water.

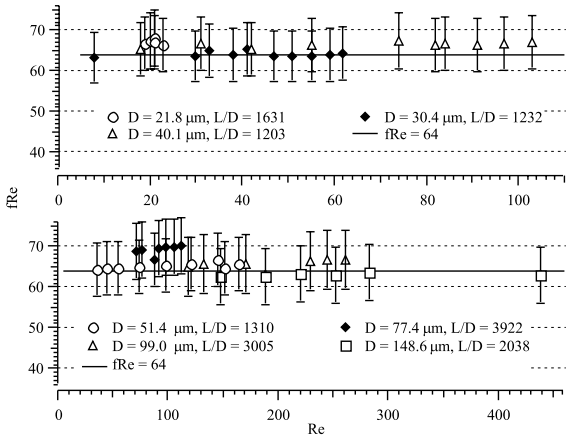

Fig. 7. Measured *fRe* as a function of Reynolds number for fused silica circular microtubes with isopropanol.

tested was 2%. The standard deviations in *fRe* for most Reynolds number series were less than 1%. The distilled water data of Fig. 6 reveal that, well within the experimental error, the data exhibit good agreement with the $fRe = 64$ line predicted by Stokes flow macroscale theory. The average value of *fRe* for all data obtained in fused silica circular tubes using distilled water was 61.9 – within 3% of the theoretical Stokes flow value. Note also that there is no evidence of transition to turbulent flow in the range $Re \leqslant 2000$, as has been reported in some previous work [3,14,17,18].

The test results from the isopropanol and methanol tests shown in Figs. 7 and 8, respectively, also demonstrate very good agreement with Stokes flow theory. All data lie well within the experimental error spanning the theoretical laminar flow friction constant $fRe = 64$. The average value of *fRe* for all fused silica circular tube

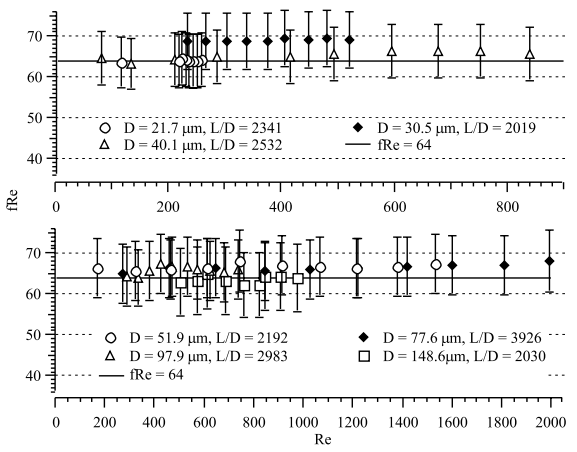

Fig. 8. Measured *fRe* as a function of Reynolds number for fused silica circular microtubes with methanol.

diameters tested over the full range of flow rates using isopropanol and methanol, respectively, were found to be 65.8 and 65.8, respectively – again within 3% of the Stokes flow theoretical value. For the range of Reynolds numbers and tube diameters tested with the fused silica microtubes, there is no evidence to suggest that fluid polarity influences the friction constant. It may be concluded that any non-Stokes phenomena present in these experiments employing fused silica circular microtubes exert influence of a magnitude which are below that bounded by the experimental uncertainty of the data.

The change in liquid viscosity with pressure, particularly for the isopropanol, was noted previously. As was indicated, increases in viscosity with increasing pressure (increasing *Re*) would have the effect of decreasing the apparent friction factor-Reynolds number product at higher *Re*. The effect would be accentuated at the higher pressures tested, which were required principally for the smaller-diameter microtubes. There is little suggestion of such a trend in Fig. 7 (isopropanol) or Fig. 8 (methanol). Values of *fRe* are nearly independent of *Re* for all diameters over the full range of Reynolds number tested. Since no pressure correction of viscosity was made in this study, the implication is that either: (i) the viscosity of liquids tested here is independent of pressure in the range investigated, or (ii) any pressure effect on viscosity is countered by other physical phenomena. The data support the former conclusion.

The frictional pressure drop data for the fused silica square microchannels tested are presented in the three panels of Fig. 9 for the distilled water, isopropanol, and methanol. The data for all three fluids agree well with the theoretical Stokes flow value of $fRe = 56.9$ for the square microchannels. The data for distilled water exhibit systematically a value of *fRe* somewhat lower than macroscale theory, but the agreement with Stokes theory is still within the estimated experimental uncertainty of approximately 10–11% for the square microchannels. Again, there is no indication of significant phenomena related to the different fluid polarities.

The stainless steel circular microtube data are presented in Fig. 10. Recall that the internal surfaces of the stainless steel microtubes were highly irregular, and determination of their diameters was subject to considerable uncertainty. Unlike the studies with the fused silica microtubes, the Reynolds number range for these stainless steel tubes exceeded $Re \approx 2000$. The data suggest evidence of a laminar-turbulent flow transition at these highest Reynolds numbers, as seen particularly in the distilled water data. The data gathered using stainless steel tubes are consistently slightly below the theoretical friction constant of $fRe = 64$. However, the uncertainty spans theory for all data. Again, if microscale phenomena proposed in previous work is at play, its influence lies within the measurable phenomena bounded by experimental error.

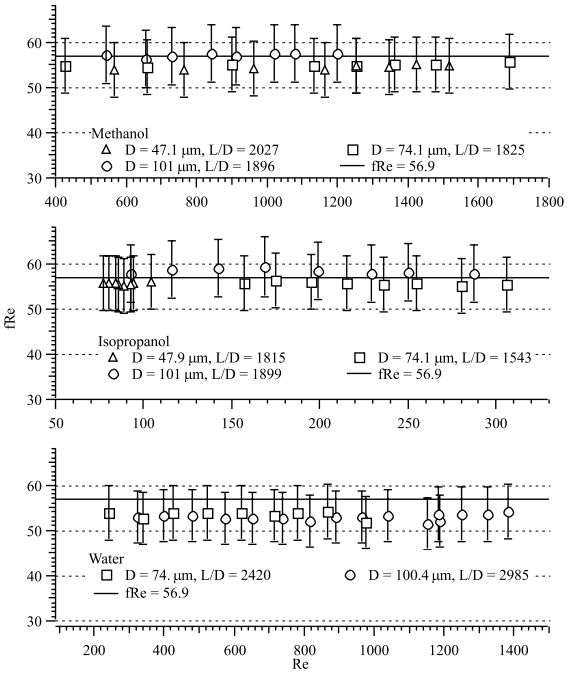

Fig. 9. Measured *fRe* as a function of Reynolds number for fused silica square microchannels, all three fluids tested.

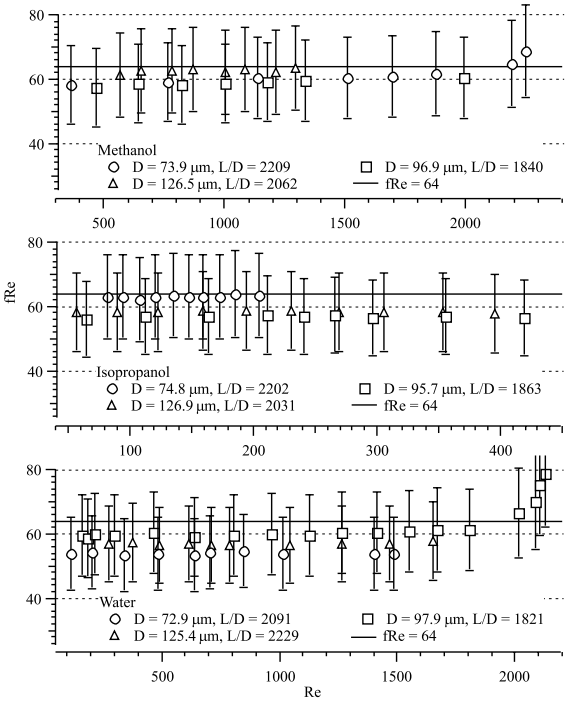

Fig. 10. Measured *fRe* as a function of Reynolds number for stainless steel circular microtubes, all three fluids tested.

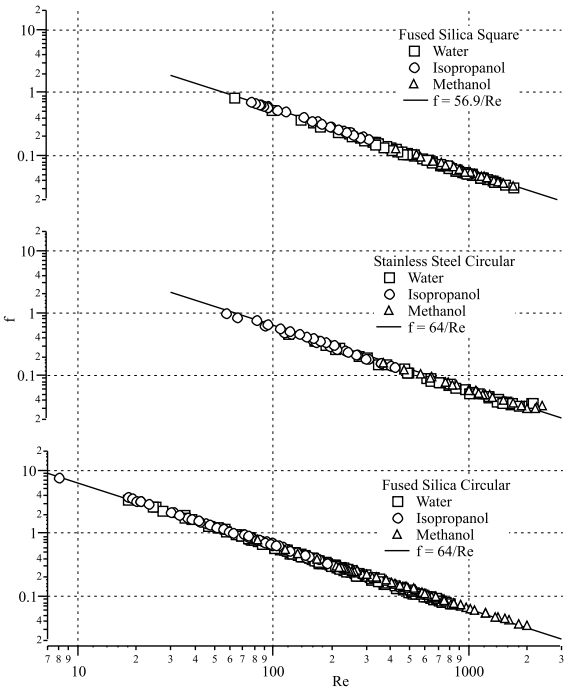

Fig. 11. Summary of f versus Re for all experimental data.

The experimental data for the fused silica circular, stainless steel circular, and fused silica square microtubes are plotted in the more classical format f versus Re in Fig. 11. The figure includes all measured data for all three fluids tested. The Stokes flow theoretical line $f = CRe$ is included, where $C = 64$ and 56.9 for the circular and square cross-section tubes, respectively. Over the two orders of magnitude variation in Reynolds number investigated ($8 < Re < 2000$), the data agree well with macroscale theory. No distinguishable differences in behavior may be seen for the three different fluids, the two microtube materials, or the two different tube cross-sections tested.

In order to explore systematic deviations in frictional pressure drop data as a function of tube hydraulic diameter, the measured friction factor-Reynolds number product normalized by the Stokes flow theoretical value $(fRe)/(fRe)_0$ is plotted as a function of hydraulic diameter in Fig. 12. Each data point in the figure represents the average of the measured fRe over the range of Re tested (where the flow regime was clearly laminar) for that specific tube diameter and for the particular fluid utilized. As was stated previously, the calculated value of fRe was nearly independent of Re (for laminar flow, $Re < 2000$) for all data, with the maximum standard deviation associated with averaging over Re being 2% for all data sets. The data of Fig. 12 show little or no systematic dependence of fRe on diameter for any fluid or microtube material combination, over the nominal

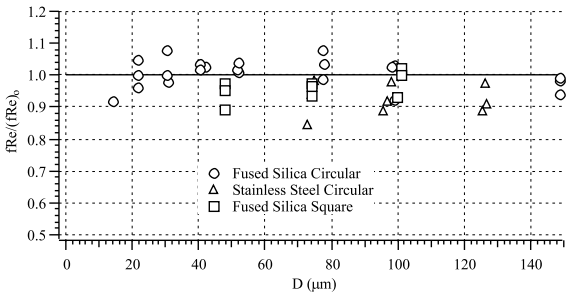

Fig. 12. Measured friction constant normalized by Stokes flow theoretical value $(fRe)/(fRe)_0$ as a function of microchannel hydraulic diameter for the three channel types tested.

diameter range investigated, $15 < D < 150$ μm. Some previous work has indicated such a dependence as D decreases due to electrokinetic [10] fluid polarity [9,21] or other phenomena [11]. While it is true that these additional phenomena may exert influence at the scale explored in this study (15–150 μm), detecting their impact is very difficult given the experimental error inherent in measurements at these scales.

It is instructive to summarize the possible sources of frictional pressure drop deviation from Stokes theory for liquid microscale flow, aside from measurement errors. There is the question of the fully-developed flow assumption. The data of this study reveal (for the range of L/D and Re investigated) that the flow does achieve a fully-developed condition. Depending on the fluid, viscous dissipation may become significant for decreasing diameter and increasing fluid velocity. The shear-induced heating of the fluid results in higher fluid temperatures along the microtube length, reducing the viscosity. Unless properly accounted for the lower viscosity can result in an apparent friction factor lower than what is expected from Stokes flow. Establishing flow in microtube environments requires high pressures. The thermophysical properties of most liquids are negligibly dependent on pressure until *ultrahigh* pressures are reached. Significantly elevated pressures result in an increase in viscosity [26,27], which would yield an apparent reduction in fRe. Pressure effects appear to be negligible in the pressure ranges explored both here and in previous work. It has also been suggested that measurement of the pressure drop between two plenums will result in an incorrect value when fRe is computed since the development region and entrance effects must be modeled with loss coefficients [31]. As summarized previously, the minor losses constitute a negligible fraction of the overall pressure drop for sufficiently large L/D and Re, as was the case in this study, and generally speaking, previous studies as well.

Electrokinetic effects have been suggested as explanations for observed deviations in frictional pressure drop at the microscale and the combination of fluid polarity and microtube material can influence these effects [32,33]. Interfacial surface chemistry suggests that for pressure-driven flows of a fluid with a very small concentration of ions an EDL will form which will subsequently result in an induced electric potential, sometimes called the streaming potential. This streaming potential will induce an electric current, termed a conduction current, in the opposite direction of bulk fluid motion and may cause a retarding of the bulk fluid motion, resulting in a lower flow rate than would otherwise exist for the imposed pressure potential. At the macroscale these effects are negligible since the size of the EDL is negligibly small as compared to the channel diameter. As the channel diameter approaches the micron scale, however, analytical studies [34] confirm that the effects of the EDL should not be neglected and can significantly contribute to the overall flow physics. However, the data of this study have revealed that despite the care taken in the experimental work the influence of such phenomena lie within the experimental error for channels of diameter 15–150 μm.

6. Conclusions

Frictional pressure drop measurements have been made over a range of Reynolds number for microtubes in the diameter range $15 < D < 150$ μm for three different fluids, two tube materials, and two different tube cross-section geometries. A careful analysis of the experimental uncertainty reveals that error bounds are dominated by measurement of the diameter. The fRe data reveal no distinguishable deviation from macroscale Stokes flow theory for any experimental condition tested. It is concluded that for the diameter range explored in this study that if non-Stokes flow phenomena exist, the influence is at a level within the experimental uncertainty.

Acknowledgements

The authors gratefully acknowledge the financial support of the U.S. National Science Foundation under Grant CTS-0085307.

References

[1] C. Ho, Y. Tai, Micro-electro-mechanical systems (MEMS) and fluid flows, Annu. Rev. Fluid Mech. 30 (1998) 579–612.
[2] J.C. Shih, C. Ho, J. Liu, Y. Tai, Monatomic and polyatomic gas flow through uniform microchannels, Microelectromech. Syst. (MEMS 59 (1996) 197–203.
[3] P. Wu, W.A. Little, Measurement of friction factors for the flow of gases in very fine channels used for microminiature

Joule–Thompson refrigerators, Cryogenics 23 (1983) 273–277.
[4] J.C. Harley, Y. Huang, H. Bau, J.N. Zemel, Gas flows in micro-channels, J. Fluid Mech. 284 (1995) 257–274.
[5] S.B. Choi, R.F. Barron, R.O. Warrington, Fluid flow and heat transfer in microtubes, Micromech. Sensors, Actuators, Syst. 32 (1991) 123–134.
[6] Z.Y. Guo, X.B. Wu, Compressibility effects on the gas flow and heat transfer in a microtube, Int. J. Heat Mass Transfer 40 (1997) 3251–3254.
[7] S.F. Choquette, M. Faghri, E.J. Kenyon, B. Sunden, Compressible fluid flow in micron-sized channels, Natl. Heat Transfer Conf. 5 (1996) 25–32.
[8] W. Urbanek, J.N. Zemel, H. Bau, An investigation of the temperature dependence of Poiseuille numbers in microchannel flow, J. Micromech. Microeng.: Struct. Dev. Syst. 3 (1993) 206–208.
[9] I. Papautsky, J. Brazzle, T. Ameel, A.B. Frazier, Laminar fluid behavior in microchannels using micropolar fluid theory, in: Sensors and Actuators, Physical Proceedings of the 1998 11th IEEE International Workshop on Micro Electro Mechanical Systems, MEMS, Heidelberg, Germany, vol. 73, 1998, pp. 101–108.
[10] G.M. Mala, D. Li, J.D. Dale, Heat transfer and fluid flow in microchannels, Int. J. Heat Mass Transfer 40 (1997) 3079–3088.
[11] J. Pfahler, J. Harley, H. Bau, J.N. Zemel, Gas and liquid flow in small channels, Micromech. Sensors, Actuators, Syst. 32 (1991) 49–58.
[12] D. Yu, R. Warrington, R. Barron, T. Ameel, Experimental and theoretical investigation of fluid flow and heat transfer in microtubes, in: Proceedings of the 1995 ASME/JSME Thermal Engineering Joint Conference, Maui, Hawaii, vol. 1, 1995, pp. 523–530.
[13] X.N. Jiang, Z.Y. Zhou, X.Y. Huang, C.Y. Liu, Laminar flow through microchannels used for microscale cooling systems, in: IEEE/CPMT Electronic Packaging Technology Conference, 1997, pp. 119–122.
[14] T.M. Harms, M. Kazmierczak, F.M. Gerner, A. Holke, H.T. Henderson, J. Pilchowski, K. Baker, Experimental investigation of heat transfer and pressure drop through deep microchannels in a (110) silicon substrate, in: Proceedings of the ASME Heat Transfer Division, vol. 1, 1997, pp. 347–357.
[15] D. Pfund, A. Shekarriz, A. Popescu, J.R. Welty, Pressure drop measurements in a microchannel, in: Proceedings of the 1998 ASME International Mechanical Engineering Congress and Exposition: DSC Micro-Electro-Mechanical-Systems, vol. 66, 1998, pp. 193–198.
[16] R.L. Webb, M. Zhang, Heat transfer and friction in small diameter channels, Microscale Thermophys. Eng. 2 (1998) 189–202.
[17] X.F. Peng, G.P. Peterson, Convective heat transfer and flow friction for water flow in microchannel structures, Int. J. Heat Transfer Mass Transfer 39 (1996) 2599–2608.
[18] X.F. Peng, G.P. Peterson, B.X. Wang, Frictional flow characteristics of water flowing through rectangular microchannels, Exp. Heat Transfer 7 (1994) 249–265.
[19] I. Papautsky, B.K. Gale, S. Mohanty, T.A. Ameel, A.B. Frazier, Effects of rectangular microchannel aspect ratio on laminar friction constant, in: Proceedings of SPIE – The International Society for Optical Engineering Proceedings of the 1999 Microfluidic Devices and Systems II , Santa Clara, vol. 3877, 1999, pp. 147–158.
[20] H.B. Ma, G.P. Peterson, Laminar friction factor in microscale ducts of irregular cross-section, Microscale Thermophys. Eng. 1 (1997) 253–265.
[21] L. Kulinsky, Y. Wang, M. Ferrari, Electroviscous effects in microchannels, in: SPIE Conference on Micro and Nanofabricated Structures and Devices for Biomedical Environmental Applications II , San Jose, CA, vol. 3606, 1999, pp. 158–168.
[22] J.R. Judy, Characterization of frictional pressure drop for liquid flows through microtubes, M.S. Thesis, Brigham Young University, 2001.
[23] Available from <http://dippr.byu.edu/public/chemsearch.asp>.
[24] R.D. Blevins, Applied Fluid Dynamics Handbook, Van Nostrand Reinhold Publishing, New York, 1984.
[25] R.C. Weast, M.J. Astle, CRC Handbook of Chemistry and Physics, CRC Press Inc., Boca Raton, FL, 1982.
[26] P.W. Bridgman, The effect of pressure on the viscosity of forty-three pure liquids, Proc. Am. Acad. 61 (1926) 57–99.
[27] P.W. Bridgman, The Physics of High Pressure, Strangeways Press Ltd., Great Britain, 1949.
[28] C.F. Poole, S.K. Poole, Chromatography Today, Elsevier, New York, 1991.
[29] C.W. Macosico, Rheology: Principles Measurements and Applications, VHC Publishers Inc., New York, 1994.
[30] C.L. Yaws, R.W. Gallant, Physical Properties of Hydrocarbons, Gulf Publishing, Houston, TX, 1993.
[31] N.T. Obot, Toward a better understanding of friction and heat/mass transfer in microchannels – a literature review, in: Proceedings of the International Conference on Heat Transfer and Transport Phenomena in Microscale, Banff Canada, 2000, pp. 72–79.
[32] G.M. Mala, C. Yang, D. Li, Electrical double layer potential in a rectangular microchannel, Colloids and Surfaces 135 (1998) 109–116.
[33] G.M. Mala, D. Li, C. Werner, H.J. Jacobasch, Y.B. Ning, Flow characteristics of water through a microchannel between two parallel plates with electrokinetic effects, Int. J. Heat Fluid Flow 18 (1997) 489–496.
[34] C.L. Rice, R. Whitehead, Electrokinetic flow in a narrow cylindrical capillary, J. Phys. Chem. 69 (1965) 4017–4024.